Multigap Superconductivity in Y_2C_3: A ^{13}C-NMR Study

A. Harada[1]*, S. Akutagawa[2], Y. Miyamichi[1], H. Mukuda[1], Y. Kitaoka[1] and J. Akimitsu[2]

[1] *Department of Materials Engineering Science, Graduate School of Engineering Science, Osaka University, Toyonaka, Osaka 560-8531, Japan*

[2] *Department of Physics and Mathematics, Aoyama-Gakuin University, Sagamihara, Kanagawa 229-8558, Japan*

(Received February 3, 2008)

We report on the superconducting (SC) properties of Y_2C_3 with a relatively high transition temperature $T_c = 15.7$ K investigated by ^{13}C nuclear-magnetic-resonance (NMR) measurements under a magnetic field. The ^{13}C Knight shift has revealed a significant decrease below T_c, suggesting a spin-singlet superconductivity. From an analysis of the temperature dependence of the nuclear spin-lattice relaxation rate $1/T_1$ in the SC state, Y_2C_3 is demonstrated to be a multigap superconductor that exhibits a large gap $2\Delta/k_BT_c = 5$ at the main band and a small gap $2\Delta/k_BT_c = 2$ at other bands. These results have revealed that Y_2C_3 is a unique multigap s-wave superconductor similar to MgB_2.

KEYWORDS: lanthanoid carbide, metal, superconductivity, multigap, NMR, Y_2C_3

The discovery of superconductivity in MgB_2, which exhibits a high superconducting (SC) transition temperature $T_c \sim 40$ K, has attracted much interest.[1] Motivated by this discovery, intensive effort is devoted to the search for a new high-T_c material in a similar system that contains light elements B and C. Meanwhile, Amano *et al*. reported that Y_2C_3 prepared under high pressure ($\sim$ 5 GPa) is a superconductor with a relatively high $T_c \sim 18$ K,[2] although the superconductivity in this compound was already reported to emerge at $T_c \sim 6-11$ K.[3] As for SC characteristics, the specific heat measurements on the newly synthesized high-purity samples of Y_2C_3 have revealed that a gap size of the respective samples with $T_c = 11.6$, 13.6, and 15.2 K increases as $2\Delta/k_BT_c$=3.6, 4.1, and 4.4.[4] This result raises a question why T_c and $2\Delta/k_BT_c$ vary significantly depending on sintering conditions. Further systematic experiments are required to gain deep insight into the SC characteristics of this compound.

Y_2C_3 crystallizes in the cubic Pu_2C_3-type structure (space group $I\bar{4}3d$) without an inversion center, consisting of the dimers of carbon atoms. The SC properties of the sample previously reported by Amano *et al*. did not exhibit a single SC transition as seen in the inset of Fig. 1(a), pointing to a contamination of extrinsic multiple phases.[2] Recently, Akutagawa *et al*. have succeeded in preparing a single phase of Y_2C_3, which enables us to extract intrinsic electronic and SC properties in Y_2C_3. From the specific-heat measurements of this sample, the Sommerfeld coefficient $\gamma \sim 6.3\,\mathrm{mJ/mol{\cdot}K^2}$ and Debye temperature $\theta_D \sim 530$ K were estimated for the sample with $T_c = 15.2$ K.[4] This result suggests that its high Debye temperature makes T_c relatively high despite its small Sommerfeld coefficient. As in MgB_2, the light-element constituent like boron and carbon plays a vital role in enhancing T_c in general. In the SC state, the temperature (T) dependence of the specific heat exhibits an exponential decrease with $2\Delta/k_BT_c = 4.4$ upon cooling well below T_c, suggesting a strong-coupling isotropic superconductivity. From an other context, it is noteworthy that a novel SC nature for $CePt_3Si$ and Li_2Pt_3B without inversion symmetry is a recent interesting topic because the admixture of spin-singlet and spin-triplet SC state is shown to emerge due to the spin-orbit coupling.[5,6] Likewise, determining the order-parameter symmetry and a detailed gap structure is an underlying issue in the newly synthesized high-quality Y_2C_3 without inversion symmetry.

In this letter, we report on the SC order-parameter symmetry and gap structure of Y_2C_3 with a relatively high $T_c = 15.7$ K ($H = 0$) via ^{13}C nuclear-magnetic-resonance (NMR) measurements under a magnetic field. Y_2C_3 was synthesized by arc melting and high pressure.[4] The sample was confirmed to nearly consist of a single phase by X-ray diffraction analyses, with the formation of a primitive Pu_2C_3-type structure. The polycrystalline sample for ^{13}C-NMR measurement was slightly enriched with ^{13}C ($^{12}C : {}^{13}C = 9 : 1$) in order to improve the NMR signal-to-noise ratio. $T_c = 15.7$ and 12.2 K were determined by ac-susceptibility measurements at $H = 0$ and 9.85 T, respectively. The NMR experiment was performed by the conventional spin-echo method at $H = 9.85$ T in the T range of $1.8 - 70$ K.

Figures 1(a) and 1(b) show the ^{13}C-NMR spectra of Y_2C_3 for the previous sample reported in ref. 2 and the present sample, respectively, in the normal state at $T = 15$ K and $H = 9.85$ T. Note that the spectra for the previous sample are composed of ^{13}C-NMR signals arising from Y_3C, YC_2, and Y_2C_3, demonstrating the contamination of extrinsic multiphases, whereas the spectra for the present sample consist of a nearly single peak from Y_2C_3 with a small contamination of YC_2. The NMR intensity for each phase coincides with the x-ray intensity as expected. The full width at half maximum (FWHM) in the ^{13}C-NMR spectrum of Y_2C_3 is as small as 8 kHz, ensuring good sample quality. Actually, a single SC transition at $T_c = 15.7$ K was corroborated by the susceptibility measurement at $H = 10$ Oe as seen in the inset of Fig. 1(b).

*E-mail address: aharada@nmr.mp.es.osaka-u.ac.jp

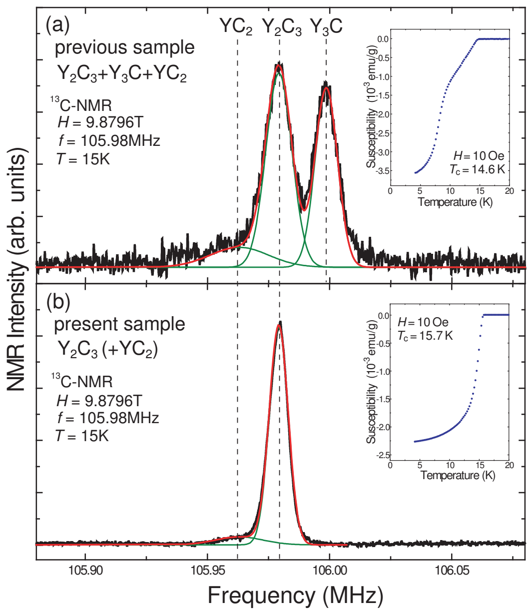

Fig. 1. (Color online) ^{13}C-NMR spectra of Y_2C_3 for (a) the previous sample reported in ref. 2 and (b) the present sample in the normal state at $T = 15$ K and $H = 9.85$ T. Note that the spectra for the previous sample are composed of NMR signals arising from Y_3C, YC_2, and Y_2C_3, demonstrating the contamination of extrinsic multiphases, whereas the spectra for the present sample nearly consist of a single peak from Y_2C_3 with a small contamination of YC_2. The insets of both figures show the T dependence of SC diamagnetic susceptibility down to 4.2 K.

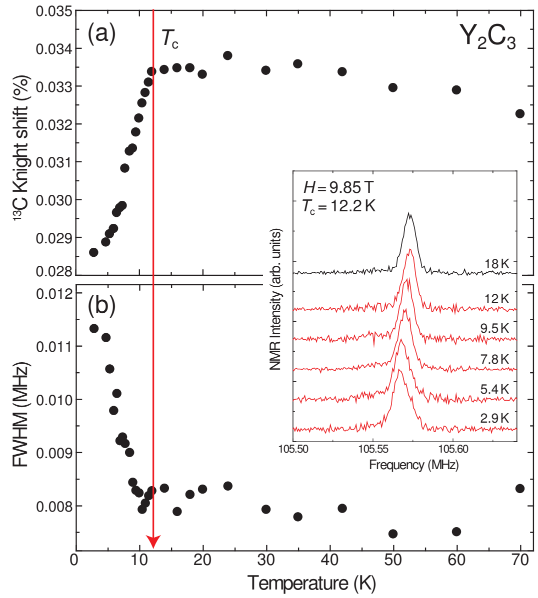

Fig. 2. (Color online) T dependences of (a) ^{13}C Knight shift and (b) full width at half maximum (FWHM) of ^{13}C-NMR spectrum in Y_2C_3 at $H = 9.85$ T. $T_c = 12.2$ K is determined by the ac-susceptibility measurement at $H = 9.85$ T as shown by an arrow pointing downward. The inset shows the NMR spectra at $T =$ 2.9, 5.4, 7.8, 9.5, 12, and 18 K, respectively.

Figure 2(a) shows the T dependence of ^{13}C Knight shift (KS) in Y_2C_3, which is determined relative to the resonance frequency of tetramethylsilane (TMS) as a reference substance (K[TMS] ~ 0 ppm). A clear decrease in KS and an increase in FWHM below T_c are indicated in Figs. 2(a) and 2(b), which are derived from the T dependence of NMR spectra as shown in the inset of Fig. 2. In intermediate fields ($H_{c1} \ll H \ll H_{c2}$) where the vortices form a dense lattice, we estimate coherence length and the distance between the vortices to be $d \sim 160$ Å, and $\xi \sim 34$ Å, respectively.[8] As a result, a diamagnetic field is led to be $H_{dia} \sim -0.3$ Oe using the relation $H_{dia} = -H_{c1}\ln(\beta e^{-1/2}d/\xi)/\ln\kappa$,[7,8] ($\kappa = \lambda/\xi$) and hence a diamagnetic shift is obtained as $K_{dia} \sim 3 \times 10^{-4}$ % at H=9.85 T. Here, we used $H_{c1} = 3.3$ mT,[4] the London penetration depth $\lambda = 4470$ Å,[4] $\beta = 0.381$ for the case of triangular lattice,[7] $d \sim 160$ Å, and $\xi \sim 34$ Å. Thus, the estimated value of K_{dia} is one order of magnitude smaller than the decrease in KS observed below T_c, demonstrating that the decrease in KS is due to the reduction of spin susceptibility associated with the onset of the spin-singlet SC state. If the spin susceptibility was assumed to vanish at low T due to the formation of spin-singlet Cooper pairing, the orbital and spin part of KS are tentatively estimated to be $K_{orb} \sim 0.028$ % and $K_s \sim 0.005$ %, respectively. A possible cause for the increase in FWHM may be due to an inhomogeneous distribution of vortex lattices, which eventually makes either d or λ distribute. Further systematic NMR measurements at low H are required for inspecting a structure of vortex lattices.

Next, we deal with the T dependence of nuclear spin-lattice relaxation rate ($1/T_1$) in order to clarify the gap structure. The $1/T_1$ for ^{13}C with nuclear spin $I = 1/2$ is uniquely determined from a simple exponential recovery curve of nuclear magnetization given by the relation $[M(\infty) - M(t)]/M(\infty) = \exp(-t/T_1)$. Here, $M(t)$ and $M(\infty)$ are the nuclear magnetizations at a time t after the saturation pulse and at the thermal equilibrium condition, respectively. Figure 3 presents the T dependence of $1/T_1$ at $H = 9.85$ T. In the normal state, the law $T_1T =$ const. is valid down to T_c. In the SC state, $1/T_1$ is also precisely measured from a simple exponential recovery curve such as $[M(\infty) - M(t)]/M(\infty) = \exp(-t/T_1)$, as seen in the inset of Fig. 4(a). This is because the possible contribution to $1/T_1$ arising from normal vortex cores is very small, if any, when $\xi \sim 34$ Å$<< d \sim 160$ Å.

The inset in Fig. 3 shows $(T_1T)_{const.}/(T_1T)$ vs T/T_c for Y_2C_3 at $H = 9.85$ T and for MgB_2 with $T_c = 29$ K at $H = 4.4$ T.[10] Here, $(T_1T)_{const.}$ denotes constant values in normal state. In the SC state, we note that a tiny coherence peak is observed in $1/T_1$ just below T_c for Y_2C_3 as in MgB_2. This is indicative of a full gap opening in Y_2C_3 as in MgB_2. A reason why the coherence peak is depressed in these compounds may be due to a strong electron-phonon coupling that causes the large life time broadening of quasiparticles induced by thermally excited phonons as reported in ref. 10. In fact, the strong-coupling BCS superconductor such as $TlMo_6Se_{7.5}$ does not show a clear coherence peak.[11] Note that the T dependence of $1/T_1$ well below T_c does not exhibit a simple exponential decrease, but seems to have a kink at around $T = 5$ K. In order to gain further insight into this unique and relevant relaxation behavior with a possible gap structure in the SC state for Y_2C_3, we present in Fig. 4 the Arrhenius plot of $(T_1T)/(T_1T)_{const.}$ vs T_c/T

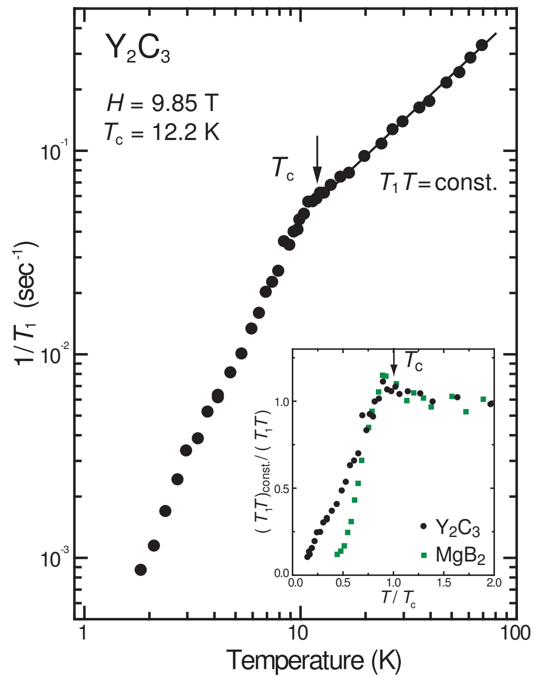

Fig. 3. (Color online) T dependence of $1/T_1$ for Y_2C_3 with $T_c = 12.2\,K$ at $H \sim 9.85\,T$. A tiny coherence peak just below T_c is observed for Y_2C_3 as in MgB_2 as shown in the inset. The inset shows the $(T_1T)_{const.}/(T_1T)$ vs T/T_c curve for Y_2C_3 (solid circles) at $H = 9.85\,T$ and for MgB_2 (solid squares) with $T_c = 29\,K$ at $H = 4.4\,T$.[10] Here, $(T_1T)_{const.}$ denotes constant values in normal state.

with $T_c = 12.2\,K$ at $H = 9.85\,T$. It is evident that a power-law behavior in $1/T_1$ such as $1/T_1T \propto T^2$ (see the dashed line in the figure) is not valid at all. Instead, when noting that a line in this plot corresponds to an exponential T dependence in $1/T_1T$, it is supposed that a large full gap seemingly opens in a high-temperature regime in the SC state, but low-lying quasiparticle excitations in a low-temperature regime are dominated by the presence of a small full gap. In fact, from respective slopes in this plot in the T range of $5\,K$-$T_c = 12.2\,K$ and at temperatures lower than $5\,K$, gap sizes are estimated to be $2\Delta/k_BT_c \sim 5$ and 2, which suggests that two kinds of SC energy gaps exist, namely, multigap superconductivity takes place in Y_2C_3. We stress that this novel relaxation behavior in the SC state for Y_2C_3 is not due to some inhomogeneous effect originating from the presence of vortex cores and/or a distribution of T_c because $1/T_1$ is uniquely determined from the simple exponential recovery curve of nuclear magnetization as shown in the inset of Fig. 4.

Here, we apply a phenomenological multigap model for nodeless superconductivity to understand the novel relaxation behavior in the SC state. Figure 5 shows the T dependence of $1/T_1T$. In such a model, $T_1(T_c)/T_1(T)$ is expressed as

$$\frac{T_1(T_c)}{T_1(T)} = \frac{\alpha^2}{\alpha^2+\beta^2}\frac{1}{T_1}(\Delta_\alpha) + \frac{\beta^2}{\alpha^2+\beta^2}\frac{1}{T_1}(\Delta_\beta),$$

where α and β are defined as the respective fractions of $N(E_F) \times A_{hf}$ with SC gap Δ_α and Δ_β and $\alpha + \beta = 1$. $N(E_F)$ and A_{hf} are the density of states (DOS) at the Fermi level and the hyperfine coupling constant, respectively. Here,

$$\frac{1}{T_1}(\Delta) = \frac{2}{k_BT_c}\int_0^\infty dE\,[N_s^2(E)+M_s^2(E)]f(E)[1-f(E)],$$

where $N_s(E)$ is the DOS, $M_s(E)$ is the anomalous DOS originating from the coherence effect inherent to a spin-singlet SC state and $f(E)$ is the Fermi distribution function.[12] Note that $N_s(E)$ and $M_s(E)$ are averaged over an energy broadening function assuming a rectangle shape with a width 2δ and a height $1/2\delta$.[13] We use $\delta/\Delta(0) = 0.3$ in the calculation. A theoretical curve based on the multigap model is actually in good agreement with the experiment using $\beta = 0.75$ and $2\Delta_\beta/k_BT_c = 5$ for the main band, and $\alpha = 0.25$ and $2\Delta_\alpha/k_BT_c = 2$ for other bands as shown by the solid curve in Fig. 5. It is notable that the large gap at the dominant Fermi surface is larger than the weak-coupling BCS value of $2\Delta/k_BT_c = 3.5$, indicating a strong electron-phonon coupling and being consistent with the specific-heat result.[4] The present ^{13}C-NMR has revealed that the superconductivity in Y_2C_3 is characterized by a large gap at the main Fermi surface and a small gap at others. This may be consistent with the band calculation which shows the presence of Fermi surfaces consisting of three dimensional multisheets due to the hybridization between Y-d derived states and antibonding C-dimers derived p-states.[9] We should pay attention to the relationship between the multigap and T_c. Although Y_2C_3 is a superconductor with no inversion symmetry, the present experiments have revealed that this noncentrosymmetric compound is a spin-singlet superconductor with full gaps at all the Fermi surfaces, and hence rules out the possibility of the admixture of spin-triplet order parameter which is the recent underlying topic for the superconductors with no inversion symmetry.

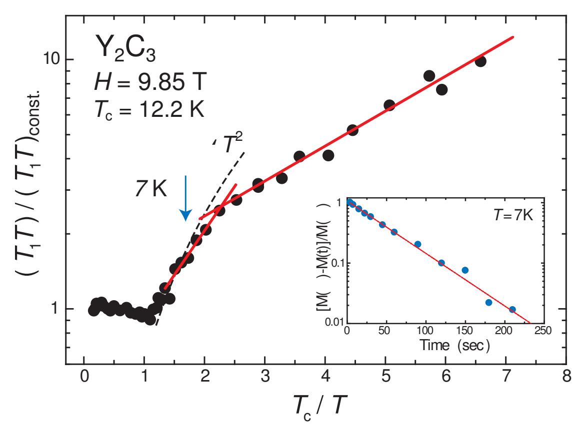

Fig. 4. (Color online) Arrhenius plot of $(T_1T)/(T_1T)_{const.}$ vs T_c/T with $T_c = 12.2\,K$ at $H = 9.85\,T$. From the respective slopes in the T range $5\,K - T_c = 12.2\,K$ and at temperatures lower than $5\,K$, gap sizes are estimated as $2\Delta/k_BT_c \sim 5$ and 2. The inset shows a simple exponential recovery curve of nuclear magnetization given by the relation $[M(\infty) - M(t)]/M(\infty) = \exp(-t/T_1)$. Here, $M(t)$ and $M(\infty)$ are the nuclear magnetizations at a time t after the saturation pulse and at the thermal equilibrium condition, respectively. Even in the SC state at $T = 7\,K$, note that $1/T_1$ for ^{13}C with nuclear spin $I = 1/2$ is uniquely determined (see the text).

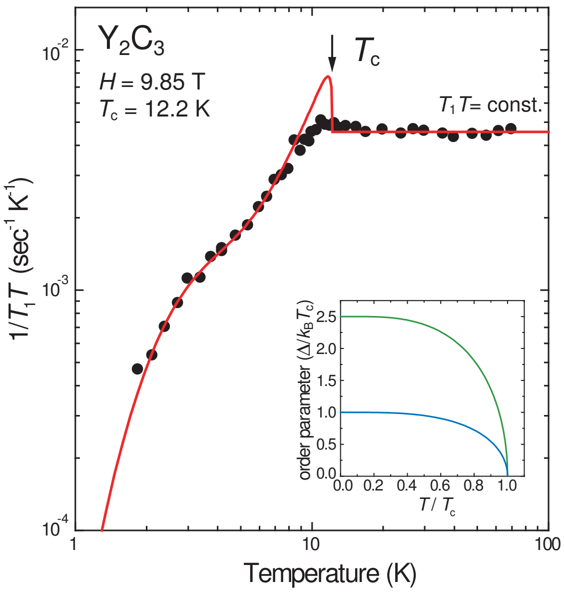

Fig. 5. (Color online) T dependence of $1/T_1T$ for Y_2C_3 with $T_c = 12.2\,K$ at $H = 9.85\,T$. A phenomenological multigap model for nodeless superconductivity is applied to understand the novel relaxation behavior in the SC state. The solid curve is a theoretical curve based on the multigap model with $\beta = 0.75$ and $2\Delta_\beta/k_BT_c = 5$ for the main band, and $\alpha = 0.25$ and $2\Delta_\alpha/k_BT_c = 2$ for other band (see the text). The inset shows the T dependences of the order parameters Δ_α and Δ_β.

In conclusion, the superconducting properties of Y_2C_3 with a relatively high transition temperature $T_c = 15.7\,K$ have been investigated using the ^{13}C nuclear-magnetic-resonance (NMR) method under a magnetic field. The Knight shift has revealed a significant decrease below T_c, suggesting the spin-singlet superconductivity. The nuclear spin-lattice relaxation study in the SC state has revealed that Y_2C_3 is a multigap superconductor that exhibits a large gap $2\Delta/k_BT_c = 5$ at the main band and a small gap $2\Delta/k_BT_c = 2$ at others. These results have revealed that Y_2C_3 is a unique multigap s-wave superconductor similar to MgB_2.

The authors would like to thank H. Kotegawa, M. Yogi, and H. Tou for fruitful discussions and comments, and N. Terasaki for experimental support. This work was supported by a Grant-in-Aid for Creative Scientific Researchi15GS0213), MEXT and the 21st Century COE Program supported by the Japan Society for the Promotion of Science.

1) J. Nagamatsu, N. Nakagawa, T. Muranaka, Y. Zenitani, and J. Akimitsu: Nature **410** (2001) 63.
2) G. Amano, S. Akutagawa, T. Muranaka, Y. Zenitani, and J. Akimitsu: J. Phys. Soc. Jpn. **73** (2004) 530.
3) M. C. Krupka, A. L. Giorgi, N. H. Krikorian, and E. G. Szklarz: J. Less-Common. Met. **17** (1969) 91.
4) S. Akutagawa and J. Akimitsu: J. Phys. Soc. Jpn. **76** (2007) No2.
5) M. Yogi, Y. Kitaoka, S. Hashimoto, T. Yasuda, R. Settai, T. D. Matsuda, Y. Haga, Y. Onuki, P. Rogl, and E. Bauer: Phys. Rev. Lett. **93** (2004) 27003.
6) H. Q. Yuan, D. F. Agterberg, N. Hayashi, P. Badica, D. Vandervelde, K. Togano, M. Sigrist, and M. B. Salamon: Phys. Rev. Lett. **97** (2006) 017006.
7) P. G. De Gennes: *Superconductivity of Metals and Alloys*, translated by P. A. Pincus (W. A. Benjamin, New York, Amsterdam, 1966).
8) We use $H_{c2} = -0.691(dH_{c2}/dT)T_c$ and $\xi^2 = \phi_0/2\pi H_{c2}$ to get the value of ξ. d is estimated using $d^2 = 2\phi_0/\sqrt{3}B$ (triangular lattice). ϕ_0 is the flux quantum.
9) D. J. Singh and I. I. Mazin: Phys. Rev. B **70** (2004) 052504.
10) H. Kotegawa, K. Ishida, Y. Kitaoka, T. Muranaka, and J. Akimitsu: Phys. Rev. Lett. **87** (2001) 127001.
11) S. Ohsugi, Y. Kitaoka, M. Kyogaku, K. Ishida, K. Asayama, and T. Ohtani: J. Phys. Soc. Jpn. **61** (1992) 3054.
12) L. C. Hebel and C. P. Slichter: Phys. Rev. **113** (1959) 1505.
13) L. C. Hebel and C. P. Slichter: Phys. Rev. **116** (1959) 79.